

Original Article

Gecko ethanol extract inhibits lymph angiogenesis through the VEGF-C/VEGFR-3 pathway *in vitro* and *in vivo*

Meng-Li Guo¹, Leng-Xin Duan¹, Cai-E Wang², Ying Jin¹, Ling Liu¹, Yi-Meng Duan¹, Jian-Gang Wang¹

¹Department of Pharmacology, Medical College, Henan University of Science and Technology, Kaiyuan Avenue 263, Luoyang 471023, Henan Province, China; ²Department of Pharmacy, The First Affiliated Hospital, College of Clinical Medicine of Henan University of Science and Technology, Luoyang 471003, Henan Province, China

Received July 11, 2017; Accepted May 7, 2018; Epub September 15, 2018; Published September 30, 2018

Abstract: Gecko ethanol extract (GEE) is an active component extracted from the gecko, and has been reported to be effective against hepatocellular carcinoma (HCC). However, its potential effects and mechanisms, by which it inhibits HCC lymph angiogenesis, are still unclear. The 3-(4,5-dimethylthiazol-2-yl)-2,5-diphenyltetrazolium bromide (MTT) assay was used to evaluate the anti-proliferative effect of GEE on human liver carcinoma HepG2 cells, and the expression level of vascular endothelial growth factor-C (VEGF-C) was detected. BALB/c mice bearing H22 hepatoma were randomly divided into model group (normal saline), control group (adriamycin, 2 mg/kg¹) and low, middle and high dose of GEE (20, 40 and 80 mg/kg¹) groups. The tumors were removed and the lymphatic micro vessel density (LMVD) was measured. Western blot and reverse transcription-PCR (RT-PCR) were used to detect VEGF-C and VEGFR-3. Results showed that GEE significantly inhibited the proliferation of HepG2, and the expression of VEGF-C decreased with increasing GEE concentration. In addition, GEE markedly inhibited transplanted tumor growth. A lower LMVD was detected in the GEE groups, and the protein and mRNA expression of VEGF-C and VEGFR-3 were also down-regulated. Our results indicate that GEE has a significant inhibitory effect on lymph angiogenesis in hepatic carcinoma. This may occur through the suppression of VEGF-C/VEGFR-3 signaling pathways.

Keywords: Gecko ethanol extract (GEE), hepatocellular carcinoma, lymph angiogenesis, VEGF-C, VEGFR-3

Introduction

Hepatocellular carcinoma (HCC), a common malignant tumor of the digestive system, is the third leading cause of cancer related death [1, 2]. Lymphatic metastasis is a factor that critically influences the progress and prognosis of HCC. Recent data shows that lymph node metastasis occurs in one third of patients with hepatocellular carcinoma [3-6]. Current treatment methods of primary liver cancer include surgery, radiation therapy, interventional therapy, hyperthermia therapy, biological therapy and liver transplantation; however, they cannot achieve the desired therapeutic effect [7, 8]. It is generally believed that, in the treatment of primary liver cancer, Chinese medicine has the unique advantages and mild and few side effects [7].

VEGF-C is the first confirmed lymphatic vascular endothelial growth factor. VEGF-C binds to

the tyrosine kinase receptor vascular endothelial growth factor receptor 3 (VEGFR-3) in lymphatic endothelial cells and then activates intracellular tyrosine phosphorylation, eliciting a series of complex signal transduction pathways. These involve the extracellular regulatory kinase ERK1/2 and phosphatidylinositol 3-kinase P13K/AKT, and promote lymphatic endothelial cell proliferation, enable migration to form new lymphatic vessels and mediate lymph node metastasis of tumor cells. A large number of studies have shown that VEGF-C and VEGFR-3 are highly expressed in human tumor tissues and closely related to the formation of lymphatic vessels and the metastasis of tumor cells.

The gecko, or ShouGong, has been widely used in traditional medicine in China [9]. Gecko extracts have been associated with effects including inhibition of multiple malignant tumors, reduce blood pressure, improve blood

supply to tissue, defense against bacteria and relief of asthma [10]. There has been increasing basic and clinical scientific evidence to support the anticancer activity of gecko extracts in recent years.

Preliminary studies have suggested that gecko ethanol extract (GEE) can inhibit the proliferation of HepG2 cells [11] and tumor growth in H22-transplanted mice [12], but its effects on tumor lymph angiogenesis and their mechanisms have not been elucidated. We investigated effects of GEE on lymph angiogenesis of HCC *in vivo* and *in vitro*. This study will also provide experimental evidence for the clinical treatment of HCC.

Materials and methods

Animals and cell lines

BALB/c mice that weighed 18-22 g were obtained from the experimental animal center of Henan University of Science and Technology, Luoyang, China (Certificate Number: 2015-0007 scxk). The present study was approved by the Animal Ethics Committee of Medical College of Henan University of Science and Technology (Luoyang, China). All experimental procedures were conducted in conformity with the National Institutes of Health Guide for Care and Use of Laboratory Animals [13].

Hepatocellular carcinoma (HepG2) cells were obtained from the Medical College of Henan University of Science and Technology.

Murine H22 hepatocarcinoma cells were obtained from the Henan Institute of Pharmaceutical Sciences (Zhengzhou, China) and cultured in Dulbecco's modified Eagle's medium (DMEM, Hyclone, USA) containing 10% fetal bovine serum (FBS, Biological Industries, Israel), penicillin (10^7 U/l, Solarbio, Beijing, China), and streptomycin (10 mg/l, Solarbio, Beijing, China). The cells were subcultured until reaching the logarithmic growth phase and then were maintained by transplanting them into the peritoneal cavities of BALB/c mice weekly.

Preparation of gecko ethanol extract (GEE) [14, 15]

The gecko used in the study was purchased from Anhui Bozhou Yonggang Co. Ltd (Bozhou, China). In brief, gecko powder (100 g) was dis-

solved in 400 mL double distilled water and made into a homogenate. The homogenate was then put into a lapping machine and ground continuously for four hours. Following centrifugation at 5000 rpm for 5 min, the precipitate was collected and extracted by soaking in 400 mL 55% ethanol solution. The supernatant solution was further concentrated using a rotary evaporator to remove ethanol, and finally lyophilized in a freeze-dryer to collect the golden extraction powder which was used in the subsequent experiments as GEE.

Cell cultures

HepG2 cells were cultured in DMEM containing 10% FBS, penicillin (10^7 U/l), and streptomycin (10 mg/l). HepG2 cells in the exponential growth phase were collected for the subsequent experiments.

MTT assay for detecting the anti-proliferative effect of GEE

The inhibition of the proliferation of HepG2 cells was measured by MTT assay *in vitro* [16]. 200 μ L of HepG2 cells in logarithmic growth phase were put into 96-well cell culture plates at a density of 2×10^4 cells/mL. The 96-well plates were then incubated for 24 h to allow the cells to attach. Following this, the HepG2 cells were treated with GEE at different concentrations (0, 0.1, 0.15, 0.2, 0.25, 0.3, 0.35 and $0.4 \text{ mg} \cdot \text{mL}^{-1}$) for 24 h, 48 h and 72 h. The 96-well plate was then put in a humidified incubator at 37°C to incubate. Four hours before the end of incubation, 15 μ L MTT ($5 \text{ mg} \cdot \text{mL}^{-1}$) was added into each well. After cultivating for another 4 h, the cell culture supernatant was discarded and 150 μ L DMSO were added into each well, and the plate was placed on a plate shaker for 10 min at room temperature. Last, absorbance (A) was measured by an ELX800 Universal Microplate Reader (Bio-Tek Instruments) at 490 nm. The inhibition rate (IR) was calculated as follows: $\text{IR}\% = [1 - A_{\text{GEE}}/A_{\text{model}}] \times 100\%$.

Western blot analysis of VEGF-C of HepG2 cells

HepG2 cells were seeded into 6-well cell culture plates with a density of 5×10^5 cells/mL to incubate for 24 h, and divided into five groups: blank group (treated with NS), control group ($2 \text{ mg} \cdot \text{kg}^{-1}$ adriamycin), low dose of GEE

GEE inhibits lymph angiogenesis through the VEGF-C/VEGFR-3 pathway

group (0.1 mg·mL⁻¹, GEEL), medium dose of GEE group (0.2 mg·mL⁻¹, GEEM), high dose of GEE group (0.4 mg·mL⁻¹, GEEH). The cells after treated were then collected and centrifuged at 12,000 rpm for 20 min, and the supernatants were collected. Total protein was measured using a BCA protein assay kit (Solarbio, Beijing). Equal amounts of protein were subjected to SDS-PAGE gel electrophoresis, and the protein was transferred to polyvinylidene fluoride (PVDF, PALL, USA) at 200 mA for 2.5 h. Next, the PVDF were blocked with 5% non-fat milk in PBST at 37°C for 1 h and incubated overnight with different primary antibodies targeting mouse β -actin and VEGF-C (Proteintech, Wuhan) at 4°C. Following this, the PVDF were incubated with the corresponding horseradish peroxidase-conjugated secondary antibody for 1 h at 37°C, and then washed with PBST another three times. Finally, the protein bands were detected using the DAB (Solarbio, Beijing) chromogenic reagent and the intensity ratios of the bands were compared with control bands.

Establishment of H22 tumor-bearing mouse model

H22 cells were transferred into the abdominal cavity of BALB/c mice to obtain tumor ascites. The H22 tumor ascites were then taken from the mice and diluted with normal saline (NS) to thoroughly dilute the cells into a suspended solution at a concentration of 1×10^7 cells/mL. To establish a murine solid tumor H22 transplantation model [17], 0.2 mL of the cell suspension was injected into the right axillary region of BALB/c mice.

H22-transplanted mice were grouped and treated with different doses of GEE

Twenty-four hours after inoculation, the H22-bearing mice were randomly assigned to five groups (n = 10): model group (treated with NS), control group (2 mg·kg⁻¹ adriamycin), GEE (L) (20 mg·kg⁻¹ in NS), GEE (M) (40 mg·kg⁻¹ in NS), GEE (H) (80 mg·kg⁻¹ in NS). Adriamycin was administered by intraperitoneal injection every second day and GEE was administered by intraperitoneal injection once daily. Each mouse was weighed daily (0.1 mL·10 g⁻¹). After 10 consecutive days of injections, subcutaneous tumors were carefully collected and weighed. The IR on tumor weight was assessed as follows:

$IR (\%) = [1 - (\text{tumor weight of tested group} / \text{tumor weight of NS group})] \times 100\%$.

The thymus and spleen of the mice were also collected and weighed. The thymus and spleen indices were assessed as follows:

Thymus index (%) = thymus weight (mg)/body weight (g) \times 10.

Spleen index (%) = spleen weight (mg)/body weight (g) \times 10.

ELISA assay of VEGF-C protein

The VEGF-C protein content of the serum of tumor bearing mice was detected using a corresponding ELISA kit (Neobioscience, China) following the instructions supplied by the manufacturer. The absorbance was measured at 450 nm using an ELX800 Universal Microplate Reader. The assay was repeated three times.

HE staining was used to observe the pathological changes of tumor tissues in mice

The H22 transplanted tumor tissues were fixed in 10% neutral formaldehyde. The washed tumor tissues were dehydrated in descending grades of ethanol and cleared in xylene, then embedded in paraffin. Sections were cut at a 5 μ m thicknesses and stained with hematoxylin and eosin (H&E), then subsequently examined using a light microscope for histopathological examination.

Immunohistochemical analysis was performed to detect the LMVD of the tumor tissue

After 48 hours in 10% neutral formaldehyde, the tumor tissue went through dehydration and transparency, and was embedded in wax. It was then sectioned at 4 μ m thickness using a microtome. Sections were then deparaffinized, stepwise dehydrated and the endogenous peroxide blocked. These sections were processed with antigen retrieval, which was achieved by boiling the slides in citrate buffer (pH 6.0) for 15 min, and then washed with PBS (pH 7.2) after natural cooling to room temperature. Sections were incubated for 60 min at 37°C with anti-VEGFR-3 antibody (Proteintech, Wuhan) at a 1:100 dilution. The sections were incubated with Max Vision™ (Maixin Biotech, Fuzhou) reagent for 15 min at room temperature after being washed with PBS (pH 7.2). They

Table 1. RT-PCR primer sequences

VEGF-C upstream	5'-ACTTGCTGTGCTTCTGTCTC-3'
VEGF-C downstream	5'-GCTCCTCCAGGTCTTTGC-3'
VEGFR-3 upstream	5'-CGAGGACGAGGGTGA-3'
VEGFR-3 downstream	5'-CAGAAGAACTGCGATGAC-3'
18S upstream	5'-CACCTACGGAACTTGTAC-3'
18S downstream	5'-GTCCCCAACTCTTAGAG-3'

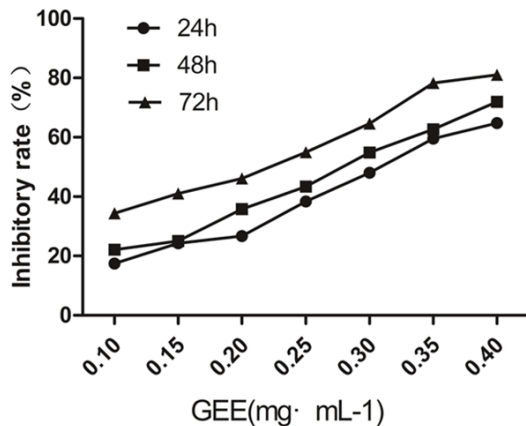


Figure 1. Inhibitory effects of GEE on the proliferation of HepG2 cells (mean \pm SD). GEE (0, 0.1, 0.15, 0.2, 0.25, 0.3, 0.35 and 0.4 mg·mL⁻¹) significantly inhibited the cell viability and proliferation.

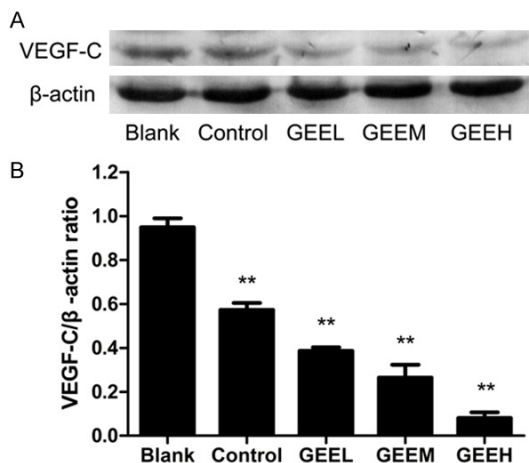


Figure 2. Inhibitory effects of GEE on the expression of VEGF-C in HepG2 cells. A. Western blot analysis of identifying VEGF-C expression in HepG2 cells. B. Ratio of the protein expression of VEGF-C to β -actin. Changes were significantly different compared with model group (** $P < 0.01$).

were then dipped in freshly prepared DAB (Solarbio, Beijing) after being washed with PBS (pH 7.2) and observed for 3-5 min under the microscope. Finally, sections were immersed in

hematoxylin and sealed in place with neutral gum. The LMVD counts were performed using the methods reported by Ohno [18] and Weidner [19] et al. Above all, the peritumoral area were observed in the low magnification ($\times 100$), the tumor (cancer nest central area) and the corresponding distal normal margin, selected the lymphatic high density area "hotspots" as measurement area, then five visual field counts were taken at random in high magnification ($\times 400$), clearly colored of individual endothelial cells as a counting unit. The cells that were unclear or blurred were not counted as counting results, and the results were expressed as an average.

RT-PCR analysis for VEGF-C and VEGFR-3 mRNA of the tumor tissue

Total RNA was extracted from 0.1 g of tumor tissues, and the purity and concentration were measured by UV spectrophotometer at A260/A280 wavelength. Reverse transcription of cDNA was performed according to the kit instructions and then amplified by PCR. Reaction conditions were: pre-denaturation at 37°C for 3 min, denaturation at 94°C for 30 s, annealing time 30 s (18 s 58°C, VEGF-C 53°C VEGFR-3 56°C), 72°C for 30 s, a total of 35 cycles, 72°C again for 3 min after the last cycle. Using 18 s as a reference, the primer sequences are shown in **Table 1**. Agarose gel electrophoresis was then performed and quantified using the Gene Genius gel imaging analysis system. The assay was repeated six times.

Western blot analysis for VEGF-C and VEGFR-3 of the tumor tissue

The tumor tissue homogenates were centrifuged at 12,000 g for 10 min, after which supernatants were collected and total protein was measured using a BCA protein assay kit. Equal amounts of protein were subjected to SDS-PAGE gel electrophoresis and the protein was transferred to PVDF at 200 mA for 2.5 h. Next the PVDF were blocked with 5% non-fat milk in PBST at 37°C for 1 h and incubated overnight with different primary antibodies targeting mouse β -actin, VEGF-C and VEGFR-3 (Proteintech, Wuhan) at 4°C. Following this, the PVDF were incubated with the corresponding horseradish peroxidase-conjugated secondary antibody for 1 h at 37°C, and then washed with

Table 2. Inhibitory effects of GEE on transplanted H22 mice (mean \pm SD, n = 10)

Group	Dosage (mg·kg ⁻¹)	Body mass (g)		Tumor mass (g)	Inhibitory rate (%)
		0 (d)	10 (d)		
Model	-	36.75 \pm 2.90	32.80 \pm 4.18	1.75 \pm 0.39	-
Control	2	35.60 \pm 2.45	33.85 \pm 4.40	0.50 \pm 0.28*	71.34
GEE (L)	20	36.92 \pm 2.30	38.92 \pm 3.41*	0.97 \pm 0.20*,#	44.67
GEE (M)	40	35.74 \pm 3.98	37.85 \pm 4.36*	0.86 \pm 0.31*,#	50.91
GEE (H)	80	36.20 \pm 2.04	38.15 \pm 3.19*	0.64 \pm 0.34*,#	63.18

Note: compared with the model group, * P <0.05; compared with the control group, # P <0.05.

Table 3. Effects of GEE on immune organs of H22 mice (mean \pm SD, n = 10)

Group	Dosage (mg·kg ⁻¹)	thymus index (mg·10g ⁻¹)	spleen index (mg·10g ⁻¹)
Model	-	2.42 \pm 0.51##	8.39 \pm 1.23##
Control	2	1.04 \pm 0.47**	3.97 \pm 1.81**
GEE (L)	20	2.37 \pm 0.53##	8.18 \pm 0.46##
GEE (M)	40	2.29 \pm 0.29##	7.96 \pm 1.04##
GEE (H)	80	1.84 \pm 0.44*,#	7.89 \pm 0.96##

Note: compared with the model group, * P <0.05,

** P <0.01; compared with the control group, # P <0.05,

P <0.01.

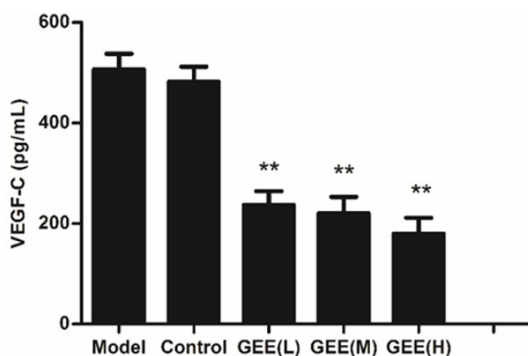


Figure 3. Effect of GEE on the protein level of VEGF-C in the mouse serum. Compared with the model group, ** P <0.01.

PBST another three times. Finally, the protein bands were detected using the DAB (Solarbio, Beijing) chromogenic reagent and the intensity ratios of the bands were compared with control bands. The assay was repeated five times.

Statistical analysis

All experimental results were expressed as the mean \pm SD. Statistical analysis was performed using SPSS 16.0 software. Differences among groups were tested by one-way analysis of variance (ANOVA). Differences were considered to

be statistically significant when P -values were less than 0.05 or 0.01 (P <0.05 or P <0.01).

Results

Inhibitory effects of GEE on the proliferation of HepG2 cells

Compared with the blank group, GEE significantly inhibited the viability and proliferation of HepG2 cells in a time- and dose-dependent manner (P <0.05, **Figure 1**). The half-maximal inhibitory concentration (IC₅₀) of GEE was 0.303, 0.257 and 0.185 mg·mL⁻¹ for 24 h, 48 h and 72 h, respectively.

GEE decreased VEGF-C protein expression in HepG2 cells

Lymph angiogenesis has been suggested as a prerequisite process for tumor growth, with VEGF-C playing an essential role in carcinoma lymph angiogenesis. The western blot result revealed that GEE could decrease VEGF-C expression levels in HepG2 cells in a dose-dependent manner, compared with the blank group (P <0.01). Groups of VEGF-C and β -actin grayscale average ratio were (94.94 \pm 4.03)%, (57.26 \pm 3.15)%, (38.65 \pm 1.59)%, (26.45 \pm 5.89)%, (8.06 \pm 2.61)% (**Figure 2**).

Inhibitory effect of GEE on tumor growth

GEE significantly decreased the growth of H22 hepatoma in mice, as evaluated by tumor mass (P <0.01, **Table 2**). The inhibitory rate in the control group, GEE (L) group, GEE (M) group and GEE (H) group was 71.34%, 44.67%, 50.91% and 63.18%, respectively. This finding suggests an anti-cancer activity of GEE *in vivo*. In addition, compared with the model group, spleen index and thymus index of the control group significantly decreased, while the GEE (L), GEE (M) and GEE (H) groups showed no significant dif-

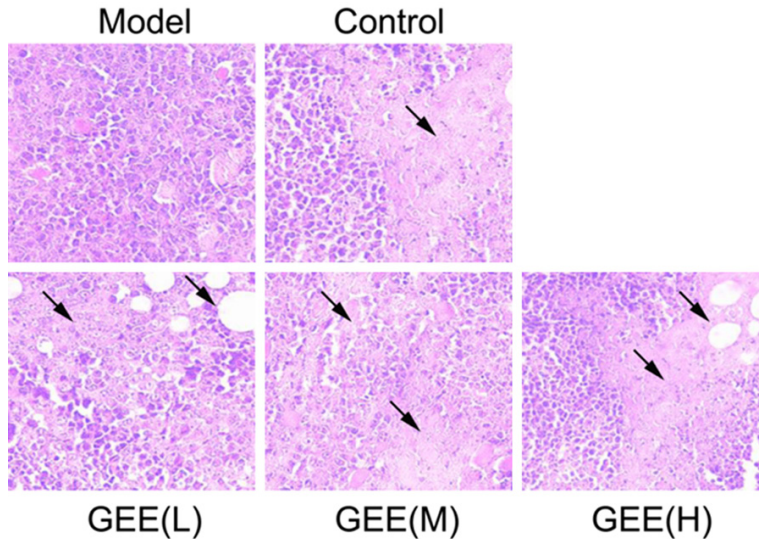


Figure 4. Pathological changes of tumor tissues in H22 mice (200 ×). The tumor tissue of the model group exhibited irregular growth, and tumor cells grew strongly and were densely arranged. In the control, GEE (L), GEE (M), GEE (H) groups, however, exhibited larger necrotic area and more vacuoles, the necrotic area was pink and the nuclei dissolved. Bar = 50 μ m.

ference ($P>0.05$). These findings suggest that GEE has no effect on the immune function of H22 hepatocarcinoma mice (Table 3).

Inhibitory effect of GEE on VEGF-C protein expression by ELISA assay

The VEGF-C level in serum of H22 hepatocarcinoma mice was detected by ELISA (Figure 3). The ELISA result showed that the VEGF-C expression levels of the GEE (L), GEE (M) and GEE (H) groups were significantly decreased compared with the model group ($P<0.01$). This result indicates that GEE can significantly inhibit the expression of VEGF-C in a dose-dependent manner.

Killing effect of GEE on mouse tumor tissues

As shown in Figure 4, the tumor tissue of the model group exhibited irregular growth, and tumor cells grew strongly and arranged densely. In the control, GEE (L), GEE (M) and GEE (H) groups, however, exhibited larger necrotic area and more vacuoles, the necrotic area was pink and the nuclei dissolved. Compared with model group, GEE (H) group had significant killing effect on tumor cells, which was higher than that of the control group.

GEE decreased LMVD in tumor tissues

Both micro-lymphatic vessels' morphological changes and LMVD of the transplanted tumor

were observed by immuno-histochemistry with VEGFR-3 antibody. The number of tumor lymphatic vessels gradually decreased in the control group and GEE (L), GEE (M) and GEE (H) groups, as the diameter of the lumen became smaller, LMVD value decreased significantly. The average LMVD value for each group was 18.9 ± 1.6 , 12.6 ± 2.3 , 14.2 ± 1.7 , 11.9 ± 2.2 and 7.6 ± 1.2 , respectively. Compared with the model group, the differences were statistically significant ($P<0.01$). The result indicates that GEE can significantly inhibit the formation of lymphatic vessels in H22 liver cancer in a dose dependent manner (Figure 5).

GEE decreased VEGF-C and VEGFR-3 mRNA and protein levels in tumor tissue

RT-PCR analysis was used to detect changes in VEGF-C and VEGFR-3 mRNA expression levels after treatment with GEE at different concentrations (20, 40 and 80 $\text{mg}\cdot\text{kg}^{-1}$). These results showed that, with increasing GEE concentration, VEGF-C and VEGFR-3 mRNA expression levels decreased ($P<0.01$) (Figure 6). Groups of VEGF-C/18S grayscale average ratio were ($52.88 \pm 1.51\%$), ($38.15 \pm 1.05\%$), ($37.01 \pm 1.17\%$), ($21.18 \pm 1.83\%$), ($14.07 \pm 1.12\%$). Groups of VEGFR-3/18S grayscale average ratio were ($51.87 \pm 1.25\%$), ($31.02 \pm 1.97\%$), ($21.34 \pm 1.98\%$), ($16.62 \pm 1.16\%$), ($10.21 \pm 1.12\%$).

Western blot analysis was used to observe the expression of lymph angiogenesis related proteins and investigate the mechanism responsible for the lymph angiogenesis induced by GEE in tumor tissue. As shown in Figure 7, western blot analysis demonstrated that VEGF-C protein expression was down-regulated compared with the model group ($P<0.01$). Groups of VEGF-C/ β -actin grayscale ratio were ($99.93 \pm 2.30\%$), ($66.11 \pm 2.16\%$), ($61.58 \pm 3.11\%$), ($59.74 \pm 4.02\%$), ($45.93 \pm 3.29\%$). Groups of VEGFR-3/ β -actin grayscale ratio were ($62.33 \pm 2.43\%$), ($25.75 \pm 3.10\%$), ($17.47 \pm 1.84\%$), ($14.43 \pm 1.22\%$), ($3.89 \pm 1.16\%$). This result

GEE inhibits lymph angiogenesis through the VEGF-C/VEGFR-3 pathway

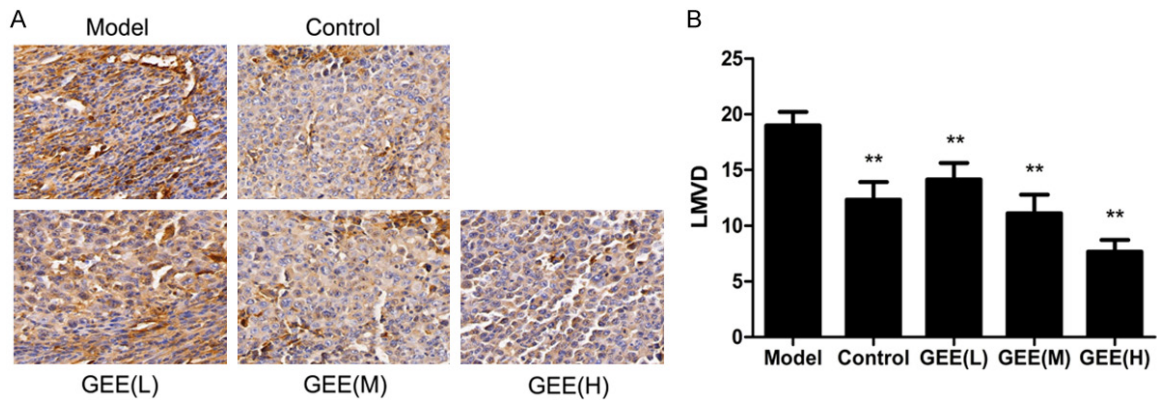


Figure 5. Immunohistochemical analysis was performed to detect the LMVD of the tumor tissue ($\times 200$). A. Protein levels of VEGFR-3 in tumor tissue assayed by immunohistochemistry. B. LMVD of the transplanted tumors was observed by immunohistochemistry with VEGFR-3 antibody. Compared with the model group, $**P<0.01$. Bar = 50 μ m.

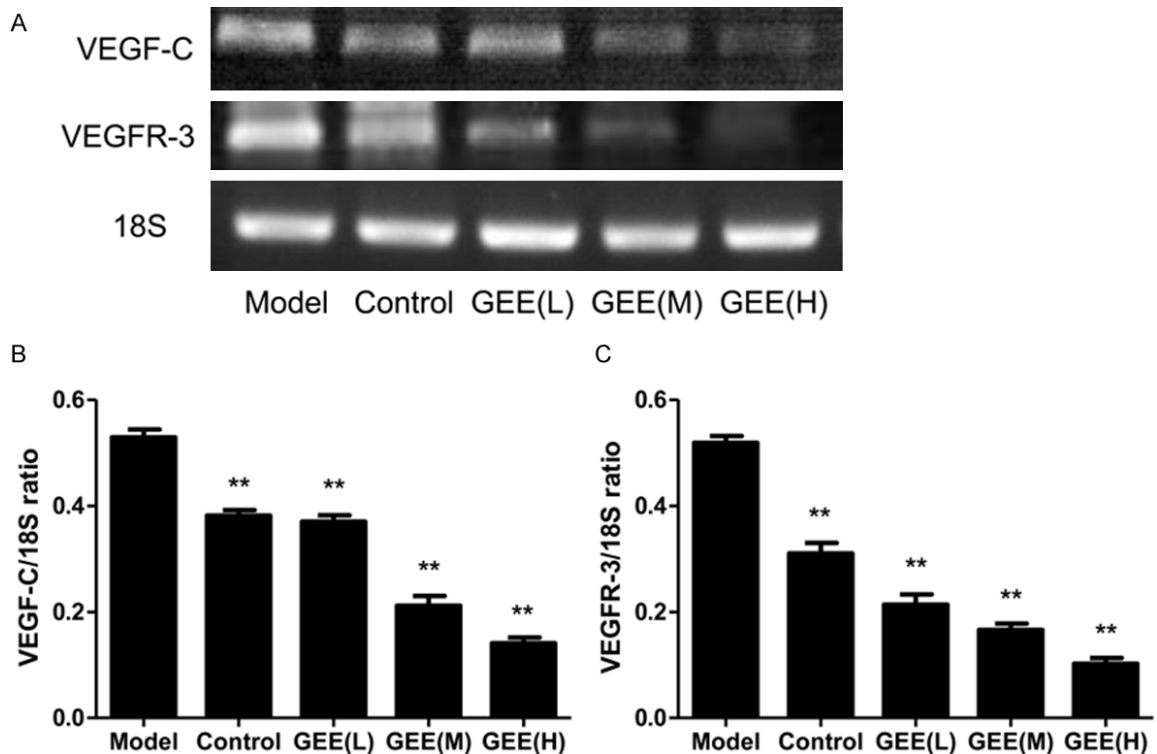


Figure 6. Effects of GEE on the expression level of VEGF-C and VEGFR-3 mRNA in tumor tissue. A. RT-PCR analysis of identifying VEGF-C and VEGFR-3 mRNA expression in tumor tissue. B. Ratio of VEGF-C mRNA expression. C. Ratio of VEGFR-3 mRNA expression. Changes were significantly different compared with the model group ($**P<0.01$).

indicates that GEE can significantly inhibit the formation of lymphatic vessels in transplanted H22 liver cancer. In addition, VEGFR-3 protein expression decreased in a dose dependent manner ($P<0.01$). These data suggest that the VEGF-C/VEGFR-3 pathway may be involved in GEE-inhibited lymph angiogenesis.

Discussion

High metastasis rate, recurrence and poor prognosis are important clinical features of hepatocellular carcinoma [20]. Lymphatic metastasis is an early event in the development of hepatocellular carcinoma [5]. Recent studies

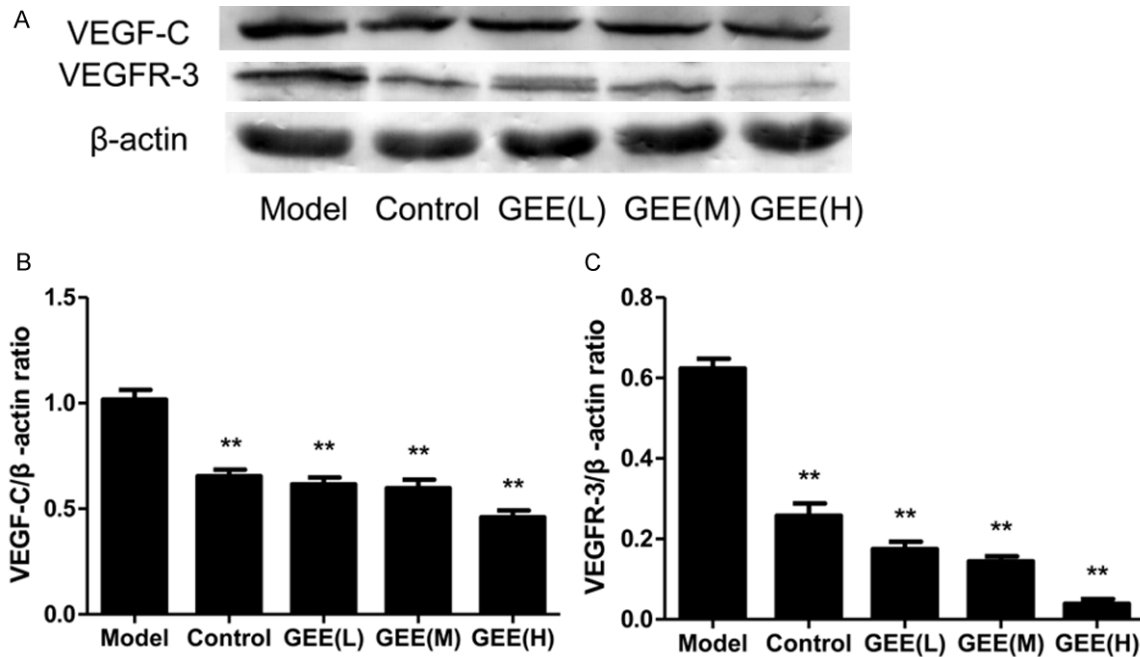


Figure 7. Effects of GEE on the expression of VEGF-C and VEGFR-3 protein. A. Western blot analysis of identifying VEGF-C and VEGFR-3 expression in tumor tissue. B. Ratio of the protein expression of VEGF-C to β -actin in tumor tissue. C. Ratio of the protein expression of VEGFR-3 to β -actin in tumor tissue. Changes were significantly different compared with the model group (** $P < 0.01$).

have confirmed that the formation of new lymphatic vessels is a necessary condition for the occurrence of lymphatic metastasis of tumors [21].

It is crucial to clearly identify micro lymphatic pathology by studying lymphatic vessels. LMVD is the measurement of lymphatic micro vessel growth in tumor, and is frequently used as a clinical indicator of lymph angiogenesis [22]. At present, frequently-used lymphatic endothelial molecular markers include VEGFR-3 [23, 24], lymphatic endothelial hyaluronic acid receptor-1 (LYVE-1) [25], mucin in glomerular mesangial cells (podoplanin) [26, 27], Prox-1 [28] and antibodies directed against M2A (D2-40) [29]. VEGFR-3 is a cell surface tyrosine kinase receptor in the lymph angiogenesis signaling pathway, and plays an important role in regulating the formation of lymphatic vessels. It is mainly expressed in lymphatic endothelial cells, and is the earliest and most widely used endothelial marker of lymphatic vessels [5, 21]. The lymphatic endothelial cells of transplanted tumor tissue were investigated by immunohistochemistry with VEGFR-3 antibody. Our results showed that the characteristics of lymphatic vessels were disorder and distortion, with

lumen expansion in the tumor-surrounding tissue of the model group. On the other hand, micro lymphatic density of transplanted tumor decreased in a dose-dependent manner in each group treated with GEE. With increasing drug concentration, the shape and structure of the lumen tended to be normal, the tube wall became regular and complete, and the diameter of the lumen became smaller.

VEGF-C, one of the key factors promoting the formation of tumor lymphatic vessels, is the most important lymphatic endothelial growth factor [30, 31]. It is highly expressed in many human malignant tumor tissues [32]. VEGF-C and its receptor VEGFR-3 form a major signal transduction pathway in the regulation of tumor lymphatic vessel formation. After binding with each other, they trigger a downstream signal transduction pathway. This promotes lymphatic endothelial cell proliferation and migration, inhibits its apoptosis and induces the formation of tumor lymphatic vessels [33, 34]. Lymphatic vessel networks around the tumor periphery are formed by increasing new lymphatic vessels, this provides more opportunity for lymphatic metastasis of tumor cells [35-41]. In addition, VEGF-C can promote the secretion

of tumor lymphatic lymph drainage and subsequent distant metastasis accompanied by lymph circulation, provide nutrients to tumor cells and promote growth of tumor cells [28]. Using experimental methods such as western blot, ELISA and immunohistochemistry, we found that GEE inhibited the VEGF-C protein expression of HepG2 cells and H22 hepatoma tumor. By RT-PCR, we further demonstrated that GEE inhibited VEGF-C and VEGFR-3 mRNA expression of H22 hepatoma tumor in a dose-dependent manner. This may indicate that GEE could significantly inhibit the production of VEGF-C and VEGFR-3 protein and the transcriptional activity of VEGF-C and VEGFR-3 mRNA in hepatocellular carcinoma. The present study demonstrated that VEGF-C/VEGFR-3 is an important target for the antitumor activity of GEE, and that GEE may inhibit lymph angiogenesis in hepatocellular carcinoma by acting on this target.

The formation of tumor lymphatic vessels is regulated by many factors and signaling pathways [42]. Studies have showed that P38-MAPK, JNK-MAPK, ERK-MAPK and PI3K/AKT are the main signal transduction pathways to regulate VEGF-C/VEGFR-3 [43]. Therefore, the VEGFR-3 signal transduction system is expected to be an effective way to treat lymphatic metastasis, and may be an ideal target for controlling tumor growth and metastasis. GEE achieved inhibition of tumor lymphatic metastasis by inhibiting the signal transduction pathway. In addition, the regulation of tumor lymphatic metastasis by GEE might be a comprehensive effect of multiple targets and multiple pathways. Therefore the anti-tumor mechanism of GEE should be explored from the aspects of molecular, cellular and animal models.

Acknowledgements

This study was supported by Medical Science and Technology Research Project of Henan Province, China, No. 102102310063. Moreover, the author thanks Louise Purtell (2014-PhD Medicine-University of New South Wales) for providing English editing.

Disclosure of conflict of interest

None.

Address correspondence to: Dr. Jian-Gang Wang, Department of Pharmacology, Medical College, Henan University of Science and Technology, Kaiyuan Avenue 263, Luoyang 471023, Henan Province, China. Tel: +86-0379-64820862; E-mail: ylwjg@163.com

References

- [1] Kumaran V. Role of liver transplantation for hepatocellular carcinoma. *J Clin Exp Hepatol* 2014; 4: S97-S103.
- [2] Lu Y, Zhu M, Li W, Lin B, Dong X, Chen Y, Xie X, Guo J and Li M. Alpha fetoprotein plays a critical role in promoting metastasis of hepatocellular carcinoma cells. *J Cell Mol Med* 2016; 20: 549-558.
- [3] Zhang L, Xiang ZL, Zeng ZC, Fan J, Tang ZY and Zhao XM. A microRNA-based prediction model for lymph node metastasis in hepatocellular carcinoma. *Oncotarget* 2016; 7: 3587-3598.
- [4] Ohtani O and Ohtani Y. Lymph circulation in the liver. *Anat Rec (Hoboken)* 2008; 291: 643-52.
- [5] Sun HC, Zhuang PY, Qin LX, Ye QH, Wang L, Ren N, Zhang JB, Qian YB, Lu L, Fan J and Tang ZY. Incidence and prognostic values of lymph node metastasis in operable hepatocellular carcinoma and evaluation of routine complete lymphadenectomy. *J Surg Oncol* 2007; 96: 37-45.
- [6] Qazi AS, Sun M, Huang Y, Wei Y and Tang J. Subcellular proteomics: determination of specific location and expression levels of lymphatic metastasis associated proteins in hepatocellular carcinoma by subcellular fractionation. *Biomed Pharmacother* 2011; 65: 407-416.
- [7] Li Y and Martin RC 2nd. Herbal medicine and hepatocellular carcinoma: applications and challenges. *Evid Based Complement Alternat Med* 2011; 2011: 541209.
- [8] Shimada K, Sakamoto Y, Esaki M, Kosuge T, Morizane C, Ikeda M, Ueno H, Okusaka T, Arai Y and Takayasu K. Analysis of prognostic factors affecting survival after initial recurrence and treatment efficacy for recurrence in patients undergoing potentially curative hepatectomy for hepatocellular carcinoma. *Ann Surg Oncol* 2007; 14: 2337-2347.
- [9] Liu F, Wang JG, Wang SY, Li Y, Wu YP and Xi SM. Antitumor effect and mechanism of gekko on human esophageal carcinoma cell lines in vitro and xenografted sarcoma 180 in Kunming mice. *World J Gastroenterol* 2008; 14: 3990-3996.
- [10] Song P, Wang XM and Xie S. [Experimental study on mechanisms of lyophilized powder of fresh gekko Chinensis in inhibiting H22 hepatocellular carcinoma]. *Chin J Integr Med* 2010; 16: 100-104.

- carcinoma angiogenesis]. *Zhongguo Zhong Xi Yi Jie He Za Zhi* 2006; 26: 58-62.
- [11] Jin Y, Duan LX, Xu XL, Ge WJ, Li RF, Qiu XJ, Song Y, Cao SS and Wang JG. Mechanism of apoptosis induction in human hepatocellular carcinoma cells following treatment with a gecko peptides mixture. *Biomed Rep* 2016; 5: 73-78.
- [12] Song Y, Wang JG, Li RF, Li Y, Cui ZC, Duan LX and Lu F. Gecko crude peptides induce apoptosis in human liver carcinoma cells in vitro and exert antitumor activity in a mouse ascites H22 xenograft model. *J Biomed Biotechnol* 2012; 2012: 743573.
- [13] U.S. National Institutes of Health. Laboratory animal welfare: Public Health Service policy on humane care and use of laboratory animals by awardee institutions; notice. *Fed Regist* 1985; 50: 19584-5.
- [14] Cui CC, Wang JG, Duan LX, Qian X and Wang CE. Apoptosis-inducing activities of gekko ethanol extract on human laryngeal carcinoma Hep2 cells. *Natural Product Research & Development* 2013.
- [15] Xu XL, Wang JG, Li RF, Li SP, Qiu XJ and Duan LX. Inhibitory effect of gecko peptides mixture on growth of human esophageal squamous carcinoma cell line EC109 cells. *Chinese Journal of Clinical Pharmacology* 2013; 29: 602-604.
- [16] Al-Sheddi ES, Farshori NN, Al-Oqail MM, Musarrat J, Al-Khedhairi AA and Siddiqui MA. Cytotoxicity of nigella sativa seed oil and extract against human lung cancer cell line. *Asian Pac J Cancer Prev* 2014; 15: 983-987.
- [17] Li H, Gu L, Zhong Y, Chen Y, Zhang L, Zhang AR, Sobol RW, Chen T and Li J. Administration of polysaccharide from panax notoginseng prolonged the survival of H22 tumor-bearing mice. *Onco Targets Ther* 2016; 9: 3433-3441.
- [18] Ohno M, Nakamura T, Kunimoto Y, Nishimura K, Chung-Kang C and Kuroda Y. Lymphagene-sis correlates with expression of vascular endothelial growth factor-C in colorectal cancer. *Oncol Rep* 2003; 10: 939-943.
- [19] Weidner N, Folkman J, Pozza F, Bevilacqua P, Allred EN, Moore DH, Meli S and Gasparini G. Tumor angiogenesis: a new significant and independent prognostic indicator in early-stage breast carcinoma. *J Natl Cancer Inst* 1992; 84: 1875-1887.
- [20] Shimada K, Sakamoto Y, Esaki M, Kosuge T, Morizane C, Ikeda M, Ueno H, Okusaka T, Arai Y and Takayasu K. Analysis of prognostic factors affecting survival after initial recurrence and treatment efficacy for recurrence in patients undergoing potentially curative hepatec-tomy for hepatocellular carcinoma. *Ann Surg Oncol* 2007; 14: 2337.
- [21] Martinez-Corral I and Makinen T. Regulation of lymphatic vascular morphogenesis: implica-tions for pathological (tumor) lymphangiogen-esis. *Exp Cell Res* 2013; 319: 1618-1625.
- [22] El-Gohary YM, Metwally G, Saad RS, Robinson MJ, Mesko T and Poppiti RJ. Prognostic signifi-cance of intratumoral and peritumoral lym-phatic density and blood vessel density in inva-sive breast carcinomas. *Am J Clin Pathol* 2008; 129: 578-586.
- [23] Mumprecht V and Detmar M. Lymphangiogen-esis and cancer metastasis. *J Cell Mol Med* 2009; 13: 1405-16.
- [24] Lohela M, Bry M, Tammela T and Alitalo K. VEGFs and receptors involved in angiogenesis versus lymphangiogenesis. *Curr Opin Cell Biol* 2009; 21: 154-165.
- [25] Jackson DG, Prevo R, Clasper S and Banerji S. LYVE-1, the lymphatic system and tumor lym-phangiogenesis. *Trends Immunol* 2001; 22: 317-21.
- [26] Schacht V, Dadras SS, Johnson LA, Jackson DG, Hong YK and Detmar M. Up-regulation of the lymphatic marker podoplanin, a mucin-type transmembrane glycoprotein, in human squamous cell carcinomas and germ cell tu-mors. *Am J Pathol* 2005; 166: 913-921.
- [27] Martin-Villar E, Scholl FG, Gamallo C, Yurrita MM, Munoz-Guerra M, Cruces J and Quintanilla M. Characterization of human PA2.26 anti-gen (T1alpha-2, podoplanin), a small mem-brane mucin induced in oral squamous cell carcinomas. *Int J Cancer* 2005; 113: 899-910.
- [28] Srinivasan RS, Dillard ME, Lagutin OV, Lin FJ, Tsai S, Tsai MJ, Samokhvalov IM and Oliver G. Lineage tracing demonstrates the venous ori-gin of the mammalian lymphatic vasculature. *Genes Dev* 2007; 21: 2422-2432.
- [29] Kaiserling E. [Immunohistochemical identifica-tion of lymph vessels with D2-40 in diagnostic pathology]. *Pathologe* 2004; 25: 362-374.
- [30] Heckman CA, Holopainen T, Wirzenius M, Kes-kitalo S, Jeltsch M, Yla-Herttuala S, Wedge SR, Jurgensmeier JM and Alitalo K. The tyrosine kinase inhibitor cediranib blocks ligand-in-duced vascular endothelial growth factor re-ceptor-3 activity and lymphangiogenesis. *Cancer Res* 2008; 68: 4754-4762.
- [31] Xu Q, Sun T, Tian H, Wang C and Zhou H. Ultra-sound-mediated vascular endothelial growth factor C (VEGF-C) gene microbubble transfec-tion inhibits growth of MCF-7 breast cancer cells. *Oncol Res* 2013; 20: 297-301.
- [32] Yu H, Zhang S, Zhang R and Zhang L. The role of VEGF-C/D and Flt-4 in the lymphatic metas-tasis of early-stage invasive cervical carcino-ma. *J Exp Clin Cancer Res* 2009; 28: 98.
- [33] Wang J, Zhang B, Guo Y, Li G, Xie Q, Zhu B, Gao J and Chen Z. Artemisinin inhibits tumor lym-

- phangiogenesis by suppression of vascular endothelial growth factor C. *Pharmacology* 2008; 82: 148-155.
- [34] Tanabe K, Shinsato Y, Furukawa T, Kita Y, Hatanaka K, Minami K, Kawahara K, Yamamoto M, Baba K, Mori S, Uchikado Y, Maemura K, Tanimoto A and Natsugoe S. Filamin C promotes lymphatic invasion and lymphatic metastasis and increases cell motility by regulating Rho GTPase in esophageal squamous cell carcinoma. *Oncotarget* 2017; 8: 6353-6363.
- [35] Lin M, Ma SP, Lin HZ, Ji P, Xie D and Yu JX. Intratumoral as well as peritumoral lymphatic vessel invasion correlates with lymph node metastasis and unfavourable outcome in colorectal cancer. *Clin Exp Metastasis* 2010; 27: 123-132.
- [36] Yang Y, Gao Z, Ma Y, Teng H, Liu Z, Wei H, Lu Y, Cheng X, Hou L and Zou X. Fucoidan inhibits lymphangiogenesis by downregulating the expression of VEGFR3 and PROX1 in human lymphatic endothelial cells. *Oncotarget* 2016; 7: 38025-38035.
- [37] Lin CC, Chen PC, Lein MY, Tsao CW, Huang CC, Wang SW, Tang CH and Tung KC. WISP-1 promotes VEGF-C-dependent lymphangiogenesis by inhibiting miR-300 in human oral squamous cell carcinoma cells. *Oncotarget* 2016; 7: 9993-10005.
- [38] Uchida Y, James JM, Suto F and Mukoyama YS. Class 3 semaphorins negatively regulate dermal lymphatic network formation. *Biol Open* 2015; 4: 1194-1205.
- [39] Hirakawa S. [New insights into the molecular mechanisms of lymphangiogenesis and pathophysiology]. *Yakugaku Zasshi* 2012; 132: 211-214.
- [40] Albrecht I and Christofori G. Molecular mechanisms of lymphangiogenesis in development and cancer. *Int J Dev Biol* 2011; 55: 483-94.
- [41] Feng Y, Hu J, Ma J, Feng K, Zhang X, Yang S, Wang W, Zhang J and Zhang Y. RNAi-mediated silencing of VEGF-C inhibits non-small cell lung cancer progression by simultaneously down-regulating the CXCR4, CCR7, VEGFR-2 and VEGFR-3-dependent axes-induced ERK, p38 and AKT signalling pathways. *Eur J Cancer* 2011; 47: 2353-2363.
- [42] Huang C and Chen Y. Lymphangiogenesis and colorectal cancer. *Saudi Med J* 2017; 38: 237-244.
- [43] Zhang P, Guo X, Li J, Yu S, Wang L, Jiang G, Yang D, Wei Z, Zhang N, Liu J and Sun Y. Immunoglobulin-like transcript 4 promotes tumor progression and metastasis and up-regulates VEGF-C expression via ERK signaling pathway in non-small cell lung cancer. *Oncotarget* 2015; 6: 13550-13563.